ELSEVIER

Physica A 244 (1997) 68–80

PHYSICA A

Formation of mesoglobules from phase separation in dilute polymer solutions: a study in experiment, theory, and applications[1]

K.A. Dawson*, A.V. Gorelov[2], E.G. Timoshenko[2], Yu.A. Kuznetsov, A. Du Chesne

Irish Centre for Colloid Science and Biomaterials, Department of Chemistry, University College Dublin, Dublin 4, Ireland

Abstract

The appearance of spherical particles resulting from heating beyond the phase separation temperature in dilute solutions of poly(N-isopropylacrylamide) has been observed by dynamic light scattering (DLS). They have a relatively narrow size distribution. The size of particles increases with increasing concentration of polymer, and decreasing heating speed. Electron microscopy confirms the existence of spherical particles with size and polydispersity in agreement with DLS. We develop a theory based on the Gaussian self-consistent method for study of the equilibrium and kinetics of conformational transitions in homopolymer solutions. The theory leads to a natural interpretation of the mesoglobules as a very long-lived metastable state. Finally, we mention the potential for these mesoglobules to find applications.

PACS: 36.20.-r; 87.15.He
Keywords: Polymer solution; Aggregate; Collapse; Phase coexistence

1. Introduction

Since the introduction of the concept of the coil-to-globule transition in polymer physics [1] the phenomenon has attracted widespread interest, both theoretical [2] and

* Corresponding author. E-mail: kenneth@fiachra.ucd.ie.

[1] This paper is presented in honour of Professor B. Widom's 70th birthday. An important part of the modern statistical mechanics has grown up under the guidance of Ben Widom and his students. In this combined experimental–theoretical paper we have tried to follow the tradition, espoused by Ben Widom, that theory and experiment can be closely tied, and that one can benefit the other. For one of us (K.A.D.) it was a privilege to work with Widom, and it is now a great honour for his scientific "son" and "grandchildren" to take part in this celebration volume.

[2] Permanent address: Institute of Theoretical and Experimental Biophysics, Russian Academy of Science, 142 292, Puschino, Moscow region.

PII S0378-4371(97)00299-9

experimental [3]. Although the contraction of chains beyond the θ-temperature has been observed many times [3], compact isolated globules have probably never been observed at equilibrium [2] for homopolymers in pure solvent. The apparent extent of contraction of the coil that is achieved varies with molecular weight and experimental conditions. It has been argued, however, that the compact state has been obtained in kinetic experiments in the presence of large aggregates [4].

Most of the early experimental work has been carried out near the upper critical solubility temperature of polystyrene in cyclohexane. In recent years there are numerous works devoted to the behaviour of water-soluble polymers near a lower critical solubility temperature (LCST). The most common systems are poly-oxyethyleneoxypropylene block copolymers and poly-N-isopropylacrylamide (PNIPAM) homopolymer, both of which have a LCST near room temperature. The phase behaviour of PNIPAM has been widely investigated in recent years (see [5] for review). It has long been noted that the LCST is relatively independent of molecular weight and concentration [6]. Again however, it has never been possible to produce isolated compact globules at equilibrium besides the case where a stable globular state has been obtained with the aid of surfactant [3]. Recently Wu and Zhou [7] obtained an 8-fold decrease in the radius of gyration for extremely dilute solutions of PNIPAM with a narrow molecular weight distribution.

In the present work we focus on the aggregation behaviour of PNIPAM near the phase separation curve using dynamic light scattering (DLS), supported by other methods such as electron microscopy. We have attempted to carefully control experiments in such a manner as to elucidate the precise nature of the phenomena in the vicinity of the transition.

At present there are few options for scientists wishing to interpret such systems. For purely equilibrium issues one can apply the Flory–Huggins theory [8]. However, it is well known that this theory is incomplete in various regimes. Approaches based on the scaling theory [9], on the self-consistent treatments in terms of the density variables [10] and on the Lifshitz theory [11] provide interesting advances. We note that the beginning of progress in the multichain problem may be observed in the recent work based on a single-mode variational approximation [12].

Here we develop a theoretical approach that is closely related to earlier ideas for the treatment of the single chain problem discussed by us [13] and others [14]. Essentially, we replace the true intra- and inter-molecular interactions by an effective harmonic interaction matrix. The set of spring constants associated with these interactions may then be adjusted to find an optimal set using some suitable criterion. The advantages of this approach include its validity for finite size systems and relative simplicity in applications to periodic and random copolymers and semiflexible polymers [15]. We emphasize that in many practical situations it may be almost impossible to access true equilibrium, and it becomes important to have a single theoretical framework that can address both equilibrium and kinetics. From this theoretical approach we can confirm and interpret the experimental observations above.

2. Dynamic light scattering and electron microscopy

For details of materials, PNIPAM polymerisation, fractionation, characterisation, DLS, electron microscopy and data analysis techniques we refer the reader to the more complete account of our work in the forthcoming companion publications to this [16,17]. In this summary we present only the essence of the experimental work, theory, and make the appropriate connections between them.

We shall denote the samples, obtained by fractionation on a gel-permeation column, with molecular weights 9.3×10^6, 3.1×10^6 and 2.0×10^6 discussed in Ref. [16] as P1, P2, P3 respectively. First we investigated the coil-to-globule transition for sample P1 with estimated polydispersity of 1.2 and concentration 2.5×10^{-5}g/cm^3. The contraction of the coil is observed above the θ-line (shown in the insert of Fig. 1) in a manner similar to that previously reported for PNIPAM [7,18]. We were able to obtain 30% decrease in the hydrodynamic radius R_h in the stable region where the scattering intensity, extrapolated to zero angle, was constant, and therefore where the aggregation was negligible. However, further increase in temperature leads to a combined collapse–aggregation process where groups of polymers collapse and aggregate together to form small, relatively monodisperse, compact globules. Given their mesoscopic nature, in order to indicate that each particle consist of many collapsed polymer chains, we have named them *mesoglobules*. We comment here that this phenomenon disappears for polydisperse polymer samples and care should be taken in preparation to ensure that chains have fairly fixed molecular weight. Upon further raising the temperature, the aggregates slightly decrease in size and finally become essentially stable with temperature. Additional experiments have shown that globules are constant in size up to 65°C. To be precise, a range of temperatures up to 65°C were studied in separate experiments. The globule size was found to be stable within the precision of the experiment during a period of days.

Our evidence for all of this is as follows. Firstly, Fig. 1 shows the **k**-dependence of the apparent diffusion constant derived from the cumulant analysis, D_{app}, for a coil near the θ-line at 30°C and for aggregates at 34.8°C. Strong dependence on the wave length reflects an increased contribution of internal motions at large **k** in the coil state. On the contrary, at 34.8°C, where aggregates are formed, D_{app} is independent of **k**. The radius, calculated from the cumulant analysis, coincides with that derived from the CONTIN analysis routine, which shows a narrow size distribution. The second cumulant of the scattering intensity drops to the value 0.02–0.06, being smaller for larger angles, reflecting, probably, the presence of some aggregates of mesoglobules.

We conclude therefore that, above the transition curve, we have solid spherical particles of relatively monodisperse size distribution. Now, a set of experiments has been carried out to examine the dependence of mesoglobule size on the heating rate. The sample P3 with concentration 1.2×10^{-4}g/cm^3 was heated from 30°C to 37°C with different speeds, and DLS studies were carried out at 37°C for each heating run.

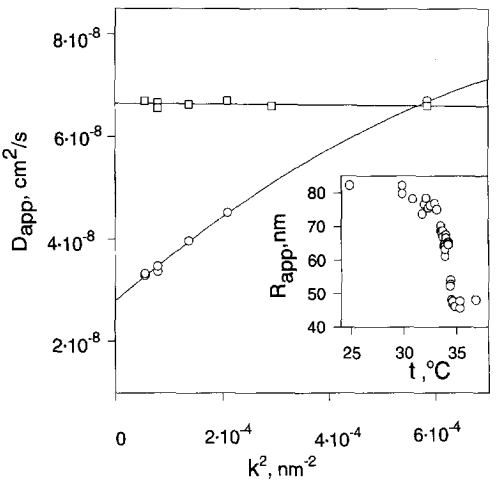

Fig. 1. Dependence of the apparent diffusion coefficient on the wave number $\mathbf{k}^2$ for sample P1. Circles and squares correspond to 30°C (Flory coil close to θ-point) and 34.5°C (mesoglobules) respectively. Insert: R_{app} as a function of temperature for sample P1. Scattering angle: 30°.

After each run, the polymer sample was then allowed to dissolve at 20°C until the initial value of R_{app}, derived from D_{app}, at low angles was recovered. We found that the size of the mesoglobules decreases with increasing heating speed [16]. We also note that, at the final temperature of 37°C, where our measurements are carried out, there are no changes in their size and scattering intensity over a period of hours.

We found that well above the transition temperature mesoglobules become very stable and do not change their size upon dilution. After long periods of time the presence of large aggregates of mesoglobules do become noticeable at low angles, but we still can collect correlation functions at larger angles and obtain a stable radius value over a period of days. Also, we note that the size of mesoglobules increases with the increase of initial concentration.

To further establish the existence of rather stable mesoglobules well above the transition temperature we have examined samples taken directly from the scattering cell by means of *electron microscopy*. We prepared mesoglobules from the sample P3 at a concentration 1.0×10^{-4} g/cm^3 and a heating speed of about 0.1°C/min. We found that addition of tungstophosphoric acid only slightly increases the diameter of mesoglobules from 81 to 84 nm. Fig. 2 shows a fairly uniform size distribution of spherical globules with a mean radius in agreement with the hydrodynamic radius R_h obtained by DLS. This means that well above the transition there is no significant amount of solvent in the mesoglobules. Specimens prepared for microscopy show well separated spherical particles when the sample is dried above the transition.

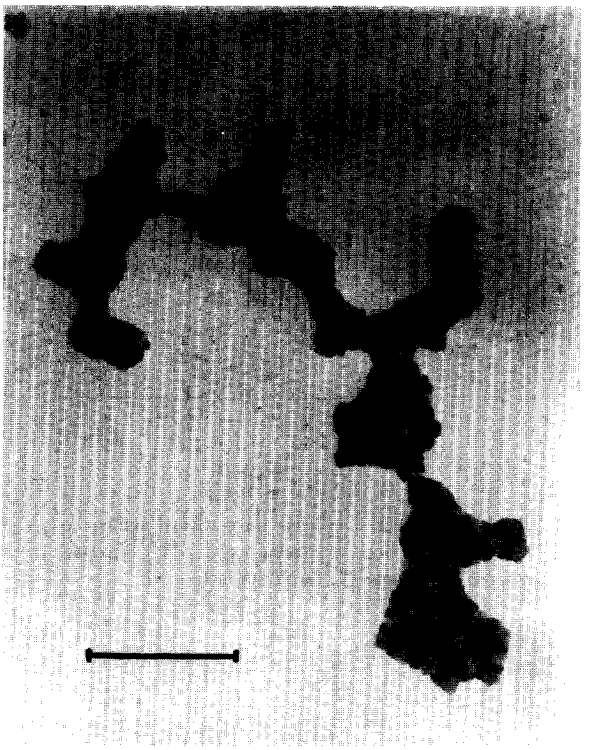

Fig. 2. Electron micrograph of mesoglobules prepared from sample P2. The details of preparation are in the text. Scale bar: 0.5 mkm. The size of mesoglobules as measured by DLS is 84 nm.

3. The multichain formalism

In this section we shall attempt to address the existence of mesoglobules from a theoretical point of view. Again, a more complete account of the theory is presented in a companion publication Ref. [16].

We shall denote by $\mathbf{X}_n^a$ the coordinates of nth monomer in the ath chain. The Langevin equation without the hydrodynamic effect is then

$$\zeta_b \frac{d}{dt}\mathbf{X}_n^a = -\frac{\partial H}{\partial \mathbf{X}_n^a} + \boldsymbol{\eta}_n^a(t)\,, \tag{1}$$

where ζ_b is the bare mobility constant of a monomer and the Gaussian noise with the second momentum proportional to $2k_BT\zeta_b$. The effective free energy functional, H, of M identical chains consisting of N monomers each is given by

$$H = \frac{k_BT}{2l^2}\sum_{a,n}(\mathbf{X}_n^a - \mathbf{X}_{n-1}^a)^2 + \frac{k_BT}{2L^2}\sum_a(\mathbf{Y}^a - \mathbf{Y})^2 + \sum_{J\geqslant 2} u_J \int d\mathbf{r}\,(\rho_v(\mathbf{r}))^J\,, \tag{2}$$

where we have written the virial expansion of the excluded volume interactions via the smoothed density, $\rho_\varepsilon(\mathbf{r}) = (\pi\varepsilon^2)^{-3/2} \sum_{a,n} \exp\left(-(\mathbf{X}_n^a - \mathbf{r})^2/\varepsilon^2\right)$, and have introduced the radii of the centre of mass of the ath chain and the whole system respectively, $\mathbf{Y}^a \equiv (1/N)\sum_n \mathbf{X}_n^a$, $\mathbf{Y} \equiv (1/M)\sum_a \mathbf{Y}^a$. The first term in (2) represents the connectivity of a chain with l being the characteristic bond length, and the second one effectively introduces a soft spatial cut-off, L, onto the system.

For simplicity we prefer to consider ring polymers, so that $\mathbf{X}_{n+N}^a = \mathbf{X}_n^a$ for any n, a, and also $\mathbf{Y}^{a+M} = \mathbf{Y}^a$ for any a. This allows us to introduce the Fourier transforms of the intra-molecular, $\mathbf{x}_q^a$ ($q \neq 0$), and the inter-molecular, $\mathbf{y}^Q$ ($Q \neq 0$), degrees of freedom possessing only the following non-vanishing equal-time correlations,

$$\frac{1}{3}\langle \mathbf{x}_q^a(t)\, \mathbf{x}_{-q}^a(t)\rangle \equiv \mathscr{F}_q(t), \quad \frac{1}{3}\langle \mathbf{y}^Q(t)\, \mathbf{y}^{-Q}(t)\rangle \equiv \frac{\Gamma^2(t)}{M}. \tag{3}$$

However, no substantial differences in the phenomena we address are expected whether we use open or ring polymers.

Proceeding along the lines Ref. [13] we arrive at the expression for the mean energy,

$$\begin{aligned}\frac{\mathscr{E}}{MN} = {} & \hat{u}_2 \left(\sum_k (D_k + \varepsilon^2)^{-3/2} + (M-1)N(2R_g^2 + 2\Gamma^2 + \varepsilon^2)^{-3/2} \right) \\ & + \hat{u}_3 \left(\sum_{k_1 \neq k_2} ((D_{k_1} + \varepsilon^2)(D_{k_2} + \varepsilon^2) - (D_{k_1,k_2} + \varepsilon^2/2)^2)^{-3/2} \right. \\ & + 3(M-1)N \sum_k ((D_k + \varepsilon^2)(2R_g^2 + 2\Gamma^2 + \varepsilon^2) - (D_k + \varepsilon^2)^2/4)^{-3/2} \\ & \left. + (M-1)(M-2)N^2 \left(\frac{3}{4}(2R_g^2 + 2\Gamma^2 + \varepsilon^2)^2 \right)^{-3/2} \right),\end{aligned} \tag{4}$$

where we have introduced the notations of Ref. [13] for the correlations of monomer positions, D_k, and the mean squared radius of gyration, R_g^2, of a chain,

$$D_k \equiv \sum_{q=1}^{N-1} d_k^{(q)} \mathscr{F}_q, \qquad R_g^2 \equiv \sum_{q=1}^{N-1} \mathscr{F}_q, \qquad d_k^{(q)} \equiv 2\left(1 - \cos\frac{2\pi q k}{N}\right), \tag{5}$$

and also $D_{k_1,k_2} \equiv \frac{1}{2}(D_{k_1} + D_{k_2} - D_{k_1-k_2})$. Similarly, for the entropy we obtain

$$\mathscr{S} = \frac{3}{2} k_B M \left(\sum_{q=1}^{N-1} \log \mathscr{F}_q - \frac{ND_1}{l^2} + \frac{M-1}{M}\left(\log \Gamma^2 - \frac{\Gamma^2}{L^2}\right) \right). \tag{6}$$

Thus, we have derived the variational free energy, $\mathscr{A} = \mathscr{E} - T\mathscr{S}$, as a function of the variables $\mathscr{F}_q$ and Γ. Its minimisation with respect to them gives the equilibrium

free energy $\mathscr{A}_{eq}$. It is also straightforward to extract the equilibrium thermodynamic functions such as the chemical potential and the osmotic pressure,

$$\mu_{eq} = \left(\frac{\partial \mathscr{A}}{\partial M}\right)_{eq}, \qquad \Pi_{eq} = -\left(\frac{\partial \mathscr{A}}{\partial L^3}\right)_{eq} = k_B T \frac{M}{L^5} \Gamma^2 . \tag{7}$$

Beginning from the Langevin equation (1) in the manner described in detail in Refs. [13,15] it is possible to derive the kinetic equations for our dynamic variables (3). These may be written as follows,

$$\frac{\zeta}{2}\frac{d}{dt}\mathscr{F}_q = -\frac{2}{3}\mathscr{F}_q \frac{\partial \mathscr{A}}{\partial \mathscr{F}_q}, \qquad \zeta \frac{d}{dt}\Gamma = -\frac{1}{3}\frac{\partial \mathscr{A}}{\partial \Gamma}, \qquad \zeta \equiv NM\zeta_b . \tag{8}$$

These equations represent, along with Eqs. (4) and (6), some of the key results of our treatment. They permit us to study both the equilibrium phase diagram and kinetics within a single theoretical treatment.

3.1. Thermodynamic limit

Now we consider the thermodynamic limit $M, L \to \infty$, $M/L^3 = const$. The free energy may be decomposed into the three parts,

$$a \equiv \lim_{L,M\to\infty} \frac{\mathscr{A}}{L^3} = a_{inter}[\Gamma] + a_{inter-intra}[\Gamma, \mathscr{F}_q] + a_{intra}[\mathscr{F}_q] . \tag{9}$$

To obtain a finite answer we should keep the concentration, $c = NM/L^3$, and the ratio $\gamma \equiv L^{-2}\Gamma^2$ finite. The inter-intra-molecular term nontrivially renormalises the interaction parameters in a_{inter}, and we obtain

$$\frac{a'_{inter}}{k_B T} = -\frac{3}{2}\frac{c}{N}\log((MN/c)^{2/3}\gamma) + \frac{3}{2}\frac{c\gamma}{N} + v_2 c^2 \gamma^{-3/2} + v_3 c^3 \gamma^{-3} , \tag{10}$$

where we have introduced the rescaled variables

$$v_J \equiv J^{-3/2}\frac{\hat{u}_J}{k_B T}\alpha_J, \quad \alpha_2 \equiv \left(1 + 3\frac{\hat{u}_3}{\hat{u}_2}\sum_k (D_k + \varepsilon^2)^{-3/2} + \cdots\right), \quad \alpha_3 = 1 . \tag{11}$$

Minimisation of (10) with respect to γ yields

$$\frac{1}{N\gamma} = \frac{1}{N} - v_2 \frac{c}{\gamma^{5/2}} - 2v_3 \frac{c^2}{\gamma^4} . \tag{12}$$

We can consider two simple limiting regimes:

(a) If $|v_2|c \ll 1/N$, $v_3 c^2 \ll 1/N$ we obtain the solution $\gamma \simeq 1 + N(v_2 c + 2v_3 c^2)$. In this regime we can solve the equations for $\mathscr{F}_q$ first, ignoring the coupling with Γ, and

substitute the result into (11)[3]. Then we obtain the Flory–Huggins expressions for the osmotic pressure and the free energy

$$\frac{\Pi_{FH}}{k_BT} = \frac{c}{N}\gamma = \frac{c}{N} + v_2c^2 + 2v_3c^3, \tag{13}$$

$$\frac{a_{FH}}{k_BT} = \frac{c}{N}\log\frac{c}{c_0} + v_2c^2 + v_3c^3, \tag{14}$$

where $c_0 = MNe^{-3/2}$ is an irrelevant constant removed by consideration of the free energy of mixing.

(b) If, on the contrary, $|v_2|c > 1/N$, i.e. N is large, we can solve (12) first ignoring the coupling in (11). The solution is

$$\gamma \simeq \left(2\frac{v_3}{|v_2|}c\right)^{2/3}.$$

This corresponds to the formation of an insoluble precipitate with the free energy and osmotic pressure,

$$\frac{a_{prec}}{k_BT} = -\frac{|v_2|^2}{4v_3}c + O\left(\frac{1}{N}\right), \qquad \frac{\Pi_{prec}}{k_BT} = \frac{c^{5/3}}{N}\left(\frac{2v_3}{|v_2|}\right)^{2/3} + O\left(\frac{1}{N^2}\right). \tag{15}$$

If we substitute the above γ back into the equations for $\mathscr{F}_q$ we shall see that the inter-chain repulsion is noticeably weakened.

3.2. Numerical analysis

We refer the reader to our earlier works [13,15] for the details[4] of the numerical procedure adopted for solving Eqs. (8).

At equilibrium we obtain the phase diagram presented in Fig. 3. For positive u_2 chains exist in the extended coil state. In the attractive regime, $u_2 < 0$, in a very narrow region at low concentrations (above and to the left of curve I′ in Fig. 3) chains collapse individually, forming a gas of non-interacting globules. The narrowness of this region is responsible for the difficulties in experimental observation of the single polymer collapse. The area below the curves I′ and II corresponds to the two phase coexistence region where $\partial^2\mathscr{A}/\partial c^2$ is negative, and point A denotes the critical point. Our treatment agrees with the Flory–Huggins theory with respect to the laws describing the boundary of the coexistence region for sufficiently small thickness parameter ε.

We may remark that the variational method allows one to obtain only pure thermodynamically dominant states, which could correspond either to stable (global minimum

[3] It is interesting to note here that at $\varepsilon = 0$ in the repulsive regime there is a strong cancellation of the two-body attraction by the inter-intra-chain three-body repulsion [16].

[4] We shall use the following choice of units of measurement: $k_BT = 1$, $l = 1$ and $\zeta_b = 1$. Also the third virial coefficient is taken equal to $u_3 = 10$.

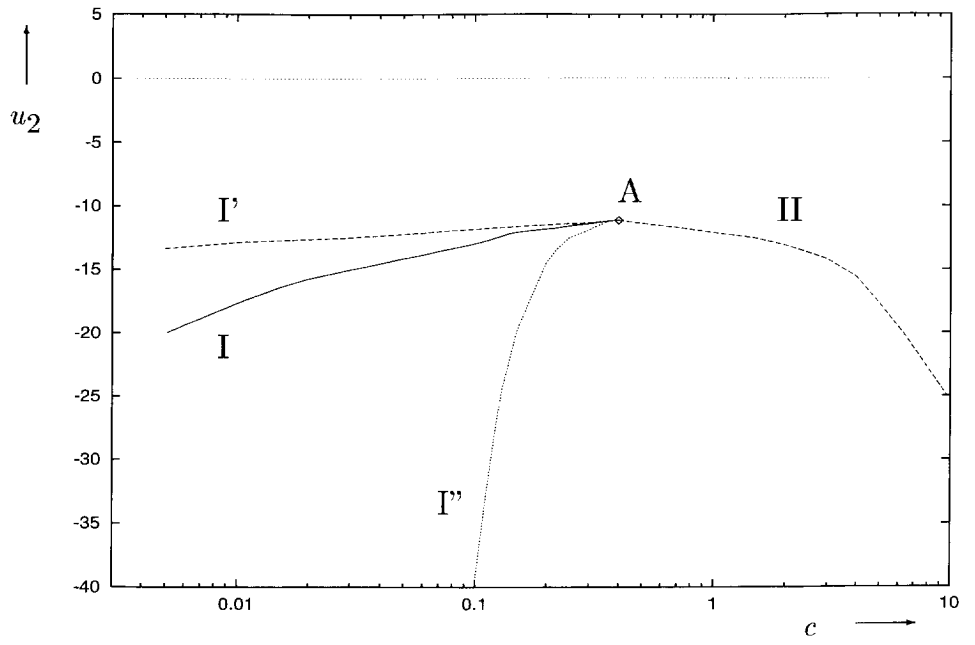

Fig. 3. The phase diagram of a homopolymer solution in variables of the concentration c and the second virial coefficient u_2. Curve I corresponds to first-order phase transition and curve II to continuous transition. Point A is a critical point. Curves I′ and I″ are "spinodals". The region of phase coexistence lies below curves I′ and II. Here $N = 100$ and $L = 100$.

of $\mathscr{A}$) or metastable (local minima) states. Thus, we have two such states here: a gas of globules above curve I, and a dense macroscopic precipitate of aggregated chains below and to the right of the first order transition curve I. Beyond curve II only the macroscopic precipitate can exist, which may be viewed simply as a macroscopic dense globular state filling most of the available space. In the region between I and the "spinodal" I″ at the same concentration the gas may exist as a metastable state, as well the metastable precipitate may exist between I and I′. The crucial observation is that $\partial^2\mathscr{A}/\partial c^2$ is negative at all of these branches in the coexistence region. Thus, we should use the Maxwell construction that joins the concave part of the free energy by a straight line. In doing so we separately treat the thermodynamically stable branches and metastable ones. This procedure results in the following picture of the two-phase coexistence region.

At equilibrium there is a coexistence of the low density gas of globules and the high-density precipitate just as in the Flory–Huggins theory. However, in the region between I and I″ there appears a metastable state formed by an interacting gas of "mesoglobules" obtained by collapse of a number of distinct chains, in principle, co-existing with a gas of single chain globules. For the mesoglobules to coalesce to a macroscopic aggregate, a potential barrier must be overcome. Thus, there should be a

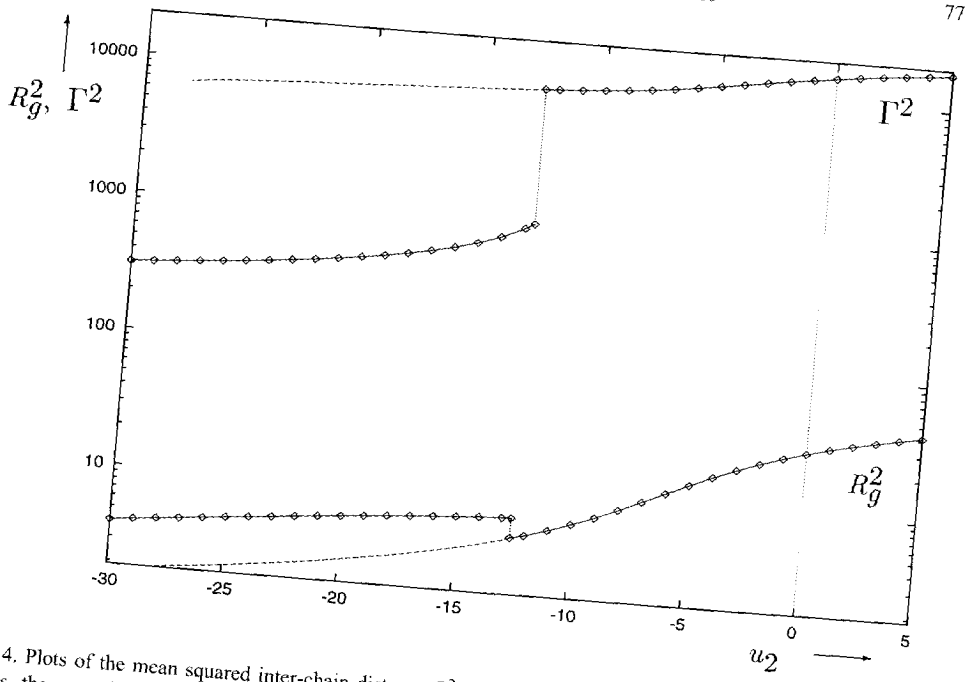

Fig. 4. Plots of the mean squared inter-chain distance Γ^2 and the mean squared radius of gyration of a chain R_g^2 vs. the second virial coefficient u_2. Here and below solid curves represent observables in the global free energy minimum and dashed curves – in metastable minima. Here $N=100$, $L=100$ and $c=0.12$.

critical size of the mesoglobules associated with the nucleation process accompanying this first-order transition. Similarly, between I and I′ there is a metastable very high density precipitate coexisting with a very low density precipitate.

In Fig. 4 we draw the quantities Γ^2 and R_g^2 across the transition curve I at different free energy branches. At I the inter-chain distance, Γ, drops dramatically from the magnitude of order L to a much smaller value corresponding to the dense precipitate with $\Gamma \sim c^{1/3}$. On the contrary, the intra-chain distance, R_g, grows markedly at the transition curve I. Really, chains tend to swell once they have formed a larger globule approaching a nearly ideal coil conformation. It is interesting to comment that R_g is very weakly dependent on the concentration c at both branches as may be established from our previous analysis.

Finally, in Fig. 5 two kinetic processes, after an instantaneous quench from the extended coil to the two phase coexistence region, are depicted. It can be seen from Eqs. (8) and (9) that the characteristic timescale of inter-chain conformational changes is of order $\zeta_b c L^2$. In our particular example the kinetics of aggregation is about 10^4 times slower than that of a single chain collapse. This may explain very long time-scales observed in some of recent experiments [4]. Also we note that the "mesoglobules" always appear in kinetics as a transient nonequilibrium state, and moreover the system may be trapped in that metastable state for a long time in kinetics after quenches to a point above "spinodal" I″.

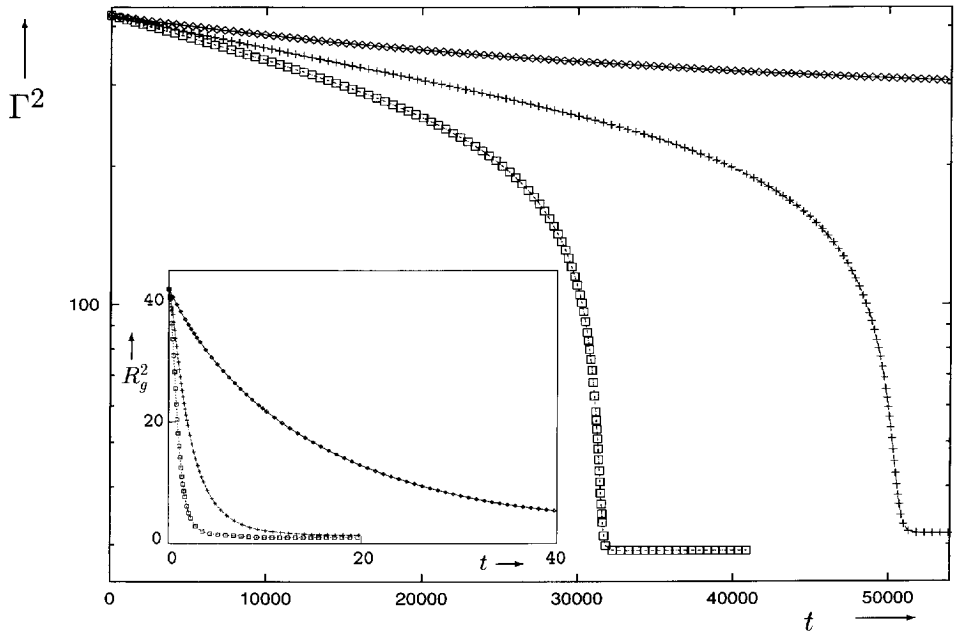

Fig. 5. Evolution of the mean squared inter-chain distance Γ^2 and the mean squared radius of gyration of a chain R_g^2 in kinetics after the quench from $u_2^{(i)} = 5$ to $u_2^{(f)} = -17$ (diamonds), -40 (pluses) and -60 (quadrangles) respectively. Here $N = 100$, $L = 20$ and $c = 0.2$.

4. Conclusion

The general conclusion of this work is as follows. We have found that, beyond the θ-point in dilute aqueous solution of PNIPAM, there exists a metastable state for the isolated contracted coil state. However, at higher temperatures dense spherical mesoglobules are observed, which are composed of a number of polymer molecules, with relatively monodisperse size distribution. We emphasise that the size of these globules may, under a broad range of circumstances, be somewhat smaller than the single molecule Flory coil state, and might in some cases be confused with an isolated collapsed globule. Our observations are confirmed by electron microscopy, where spherical globules are observed with sizes that are in fair agreement with the DLS data.

To interpret these experimental observations we have constructed a fundamental theory of multichain polymer systems for both good and poor solvent conditions. This approach permits us to study the microstructure and the kinetic phenomena. In some cases our method leads to the well known Flory–Huggins theory of polymer solutions, thereby providing a rational route to that set of results. However, we can find more rich phenomena that are of considerable interest in more realistic experimental situations. For instance it is possible to form metastable very long-lived aggregates, which we believe are the mesoglobules observed in our experiments. We note that such a state

always appears as a transient nonequilibrium state after a quench to the poor solvent region. This state is kinetically arrested since the coalescence time of solid-like particles is rather large compared to a characteristic time of their collisions. Moreover, we argue that the true equilibrium state may be very hard to reach, and thus the mesoglobules should commonly be observed in typical experiments at reasonably low dilutions. The issue of their monodispersity has not been theoretically studied at present, and we hope to return to it at a later date.

A heuristic explanation for these mesoglobules is by no means simple, an observation that lends support to the need for theory. However, roughly speaking, we can imagine the chains in solution rapidly becoming "sticky" after heating above the transition curve. The process of co-condensation of nearby chains is quite intuitively clear as the system optimises its interaction energy, losing chain entropy as the process continues. Some translational entropy of the chains is retained however because the mesoglobules themselves can move. The competition of these terms yields the metastable state. An important question remains whether the phenomenon of mesoglobules relative monodispersity is unique for PNIPAM, or it is universal for water soluble polymers with LCST.

There are a number of interesting ramifications of this work. Firstly, the conventional Flory–Huggins picture may be incomplete for many polymer-solvent systems. Mesoglobules may be ubiquitous. Secondly, one attractive practical implication of the present work is the possibility to obtain latex-like particles of controlled size, which could be redissolved upon changes in temperature or other conditions. Thirdly, it is now within the realm of theory to study simultaneously the equilibrium and kinetics of crossing phase boundaries in polymer systems. This opens the possibility to study, theoretically, a variety of fields in soft matter that have hitherto being blocked.

Acknowledgements

The authors acknowledge interesting discussions with Professors B. Chu, P.G. de Gennes, A.Yu. Grosberg, A.R. Khokhlov, P. Pincus, Y. Rabin and Dr O. Vasil'ev.

References

[1] W.H. Stockmayer, Makromol. Chem. 35 (1960) 54.

[2] O.B. Ptitsyn, A.K. Kron, Y.Y. Eizner, J.Polym. Sci. Polym. Phys. Ed. 16 (1968) 3509; P.G. de Gennes, J. Phys. Lett. 39 (1978) L299; F. Tanaka, J. Chem. Phys. 82 (1985) 4707; B. Duplantier, J. Phys. (Paris) 43 (1982) 991; Europhys. Lett. 1 (1986) 491; A.Yu. Grosberg, D.V. Kuznetsov, Macromolecules 26 (1993) 4249.

[3] S.-T. Sun, I. Nishio, G. Swislow, T. Tanaka, J. Chem. Phys. 73 (1980) 5971; M. Meewes, J. Rička, M. de Silva, R. Nyffenegger, T. Binkert, Macromolecules 24 (1991) 5811; B. Chu, R. Xu, J. Zhuo, Macromolecules 21 (1988) 273; B. Chu, Z. Wang, Macromolecules 21 (1988) 2283, J. Yu, Z. Wang, B. Chu, Macromolecules 25 (1992) 1618; I.C. Sanchez, J. Phys. Chem. 93 (1989) 6983.

[4] B. Chu, Q. Ying, A.Yu. Grosberg, Macromolecules 28 (1995) 180.

[5] H.G. Schild, Progr. Polym. Sci. 17 (1992) 163.

[6] S. Fujishige, K. Kubota, I. Ando, J. Phys. Chem. 93 (1989) 3311.
[7] C. Wu, S. Zhou, Macromolecules 28 (1995) 8381.
[8] P.J. Flory, J. Chem. Phys. 10 (1942) 51; M.L. Huggins, Ann. N.Y. Acad. Sci. 43 (1942) 1 M. Muthukumar, J. Chem. Phys. 85 (1986) 4722.
[9] M. Daoud, G. Janninck, J. Phys. (Paris) 37 (1976) 973; M. Daoud, J. Polym. Sci. Polym. Symp. 61 (1977) 305.
[10] P.G. de Gennes, Scaling Concepts in Polymer Physics, 3rd printing, Cornell University Press, Ithaca, NY, 1988; J. des Cloizeaux, G. Jannink, Polymers in Solution, Clarendon Press, Oxford, 1990; M. Doi, S.F. Edwards, The Theory of Polymer Dynamics, Oxford Science, New York, 1989; A.Yu. Grosberg, A.R. Khokhlov, Statistical Physics of Macromolecules, AIP, NY, 1994; P.J. Flory, Principles of Polymer Chemistry, Cornell University, Ithaca, 1953.
[11] A.Yu. Grosberg, D.V. Kuznetsov, Macromolecules 25 (1992) 1991; J. Phys. II (France) 2 (1992) 1327.
[12] G. Raos, G. Allegra, J. Chem. Phys. 104 (1996) 1626.
[13] E.G. Timoshenko, K.A. Dawson, Phys. Rev. E 51 (1995) 492; E.G. Timoshenko, Yu.A. Kuznetsov, K.A. Dawson, J. Chem. Phys. 102 (1995) 1816; Yu. A. Kuznetsov, E.G. Timoshenko, K.A. Dawson, J. Chem. Phys. 104 (1996) 3338.
[14] G. Allegra, F. Ganazzoli, J. Chem. Phys. 83 (1985) 397; F. Ganazzoli, R. La Ferla, G. Allegra, Macromolecules 28 (1995) 5285; E. Pitard, H. Orland, unpublished.
[15] E.G. Timoshenko, Yu.A. Kuznetsov, K.A. Dawson, Phys. Rev. E 53 (1996) 3886; Phy. Rev. E 54 (1996) 4071; Yu.A. Kuznetsov, E.G. Timoshenko, K.A. Dawson, J. Chem. Phys. 103 (1995) 4807; J. Chem. Phys. 105 (1996) 7116.
[16] A.V. Gorelov, A. Du Chesne, K.A. Dawson, Physica A 240 (1997) 443; E.G. Timoshenko, Yu.A. Kuznetsov, K.A. Dawson, Physica A 240 (1997) 432.
[17] A.V. Gorelov, L.N. Vasil'eva, A. du Chesne, E.G. Timoshenko, Yu.A. Kuznetsov, K.A. Dawson. Il Nuovo Cimento D16 (1994) 711.
[18] K. Kubota, S. Fujishige, I. Ando, J. Phys. Chem. 94 (1990) 5154; I. Yamamoto, K. Iwasaki, S. Hirotsu, J. Phys. Soc. Japan 58 (1989) 210.